Limits to the magnitude of capacitance in carbon nanotube array electrode based electrochemical capacitors

Hidenori Yamada[1,a)] and Prabhakar R. Bandaru[1,2,b)]
[1]*Department of Electrical and Computer Engineering, University of California, San Diego, La Jolla, California 92093, USA*
[2]*Program in Materials Science, Department of Mechanical Engineering, University of California, San Diego, La Jolla, California 92093, USA*

(Received 25 February 2013; accepted 18 April 2013; published online 3 May 2013)

Nanostructured electrochemical capacitors (ECs) are advantageous for charge and energy storage due to their intrinsically large surface area, which contributes to a large electrostatic/double layer capacitor (C_{dl}). However, the intrinsically small density of states in nanostructures results in a quantum capacitor (C_Q) in series with C_{dl} which could diminish the total device capacitance value (C_{tot}). We investigate, through comparison with experiment, the relative magnitudes of C_{dl} and C_Q in electrodes constituted of carbon nanotube arrays. Consequently, we attribute the increase in C_{tot} resulting from ionizing radiation to an increase in C_Q and suggest limits to the capacitance in ECs.
 [http://dx.doi.org/10.1063/1.4803925]

Electrochemical energy storage may be broadly classified as encompassing either batteries or electrochemical capacitors (ECs). While the former category incorporates devices with high energy density (~100 Wh/kg) and relatively low power density (~1 kW/kg), the latter comprises media with opposite attributes, i.e., relatively lower energy density (~10 Wh/kg) and higher power density (~10 kW/kg).[1,2] The overarching imperative is then to devise *intermediate* ECs, combining the best of both energy and power densities. Moreover, characteristics such as a high cycle life, i.e., the capability of rapid charging and discharging, for millions of cycles must be incorporated.

Much EC work has focused on charge storage in a *double layer* comprised of the electrode charge and electrolyte charge of opposite polarity—Fig. 1. Double layer capacitance/unit area (C_{dl}) is directly proportional to the dielectric constant ($\varepsilon = \varepsilon_o \varepsilon_r$, where ε_o is the permittivity of free space and is equal to 8.854×10^{-12} F/m and ε_r is the relative permittivity, e.g., ~80 for water) and inversely proportional to the charge separation distance between the positive (+) and negative (−) charges. C_{dl} is further constituted of a *Helmholtz* capacitor, where distances are of the order of the electrolyte ionic diameters, as well as a *diffusive* capacitor, with mean distances of the order of the Debye length[3] $d = \sqrt{\frac{\varepsilon k_B T}{2N_A (ze)^2 I}} \sim 9.78 \frac{1}{\sqrt{I}}$ nm, where k_B ($=1.38 \times 10^{-23}$ J/K) is the Boltzmann constant, T is the absolute temperature (K), N_A ($= 6.02 \times 10^{23}$ atoms/mole) is the Avogadro number, (ze) is the net charge with e as the elementary electronic charge ($=1.6 \times 10^{-19}$ C), and I (in moles/m^3) is the electrolyte concentration. For an aqueous electrolyte (at 1 M concentration), C_{dl} could then *potentially* be of the order of 250 μF/cm^2. The utilization of a high surface area electrode substrate, e.g., carbon nanotubes (CNTs), where the total surface area would be much larger[4] than the projected area would also be beneficial. However, the values reported in literature are typically an order of magnitude lower,[5] and this has been tentatively ascribed to incomplete/inadequate utilization of the surface area.[6] A substantial addition to total capacitance (C_{tot}) through the utilization of *parallel* redox capacitance/pseudocapacitance (C_p), which mimics battery like behavior,[7] could also be obtained in ECs as discussed in a previous study.[8,9] It was found that ion irradiation, facilitated through plasma processing, increased the observed C_{tot} value. However, details of the underlying mechanisms were not specified. In this article, we propose a possible mechanism through detailed comparison with experiment and seek to understand the limits of capacitance that may be manifested with a given CNT configuration. The underlying principles may be adapted to other nanostructure and device types as well.

We considered quantum capacitance (C_Q), which is relevant when nanostructures such as CNTs, with a finite density of states (DoS) $D(E)$, as depicted in Fig. 2. The increase (decrease) of the Fermi energy (E_F) of the CNTs could be significant, relative to the bulk electrolyte, when charge carriers

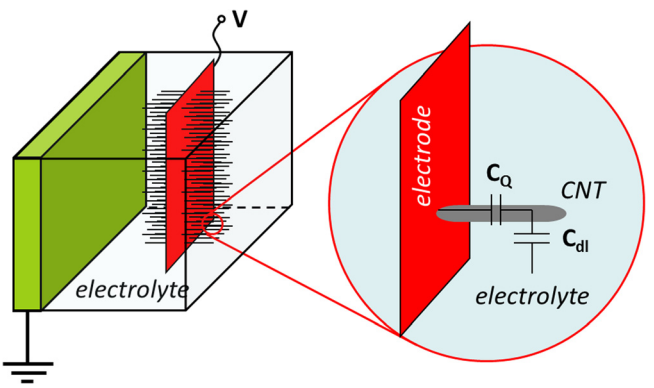

FIG. 1. A schematic of electrode configuration in an electrochemical capacitor, zoomed into a section of the CNT array. C_Q and C_{dl} in series represented within a single CNT. As the surface area for the CNT electrode (in red) is much higher than that of the counter electrode (in green), the capacitance value of the former is much more significant.

a)Electronic mail: hyamada@ucsd.edu
b)Electronic mail: pbandaru@ucsd.edu

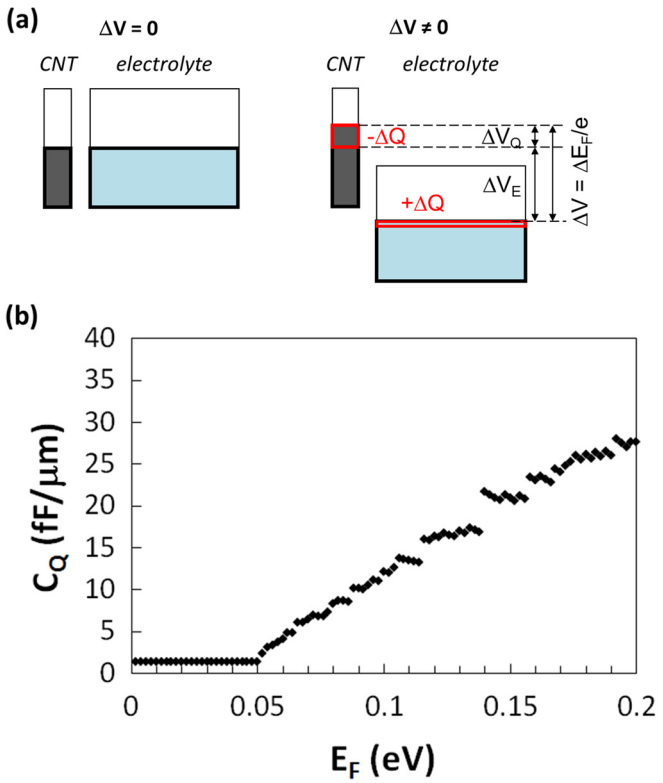

FIG. 2. (a) Representation of CNT DoS and electrolyte DoS (as columns) along with their respective Fermi energies (E_F) at equilibrium, with no applied voltage ($\Delta V = 0$)—*left figure*, and with a non-zero applied voltage ($\Delta V \neq 0$)—*right figure*. The *applied* ΔV causes a change in E_F (ΔE_F) and is partitioned between the CNT electrode (ΔV_Q) and the bulk electrolyte (ΔV_E). While ΔV_Q would be associated with C_Q, ΔV_E is related to C_{dl}. (b) C_Q as a function of E_F in a MWCNT with 15 walls. The initially flat segment of C_Q is caused by the metallic CNT walls. The staircase-like structure arises from the contributions of successive sub-bands to the DoS.

of a single type, e.g., electrons of magnitude dQ ($= e{\cdot}dn$), are added (removed) due to an applied voltage change (dV).[10] An effective capacitance could therefore be defined for a given electrode, considering the DoS at the E_F, as follows:

$$C_Q = \frac{dQ}{dV} = \frac{edn}{\frac{1}{e}dE_F} = e^2 D(E_F). \tag{1}$$

We model the *net* device capacitance in Fig. 1 as a series combination of C_{dl} *and* C_Q. If, as hypothesized,[8,11] the role of ion irradiation (e.g., through plasma processing) was to introduce fixed charges, then C_Q increases significantly with increasing processing time. The series combination of C_Q and C_{dl} would allow an increase in C_{tot} consistent with the experiment as can be understood through

$$\frac{1}{C_{tot}} = \frac{1}{C_{dl}} + \frac{1}{C_Q}. \tag{2}$$

It should be pointed out that our work focuses on correlating capacitance contributions from multi walled CNTs (MWCNTs) (with concentric nanotubes of gradually decreasing perimeters) while previous works, e.g., by Fang *et al.*[12] and Xia *et al.*,[13] are on graphene sheets or nanoribbons, the latter of which have sub-bands due to the finite width and become graphene sheets in the infinite width limit. The C_Q values of nanoribbons and graphene were discussed in Ref. 12 for MOSFET (metal oxide semiconductor field effect transistor)-like devices. While they discussed the series addition of the gate oxide capacitance and C_Q, we discuss the series addition of C_{dl} with C_Q, as appropriate for an electrochemical capacitor. The maximum carrier concentration (n) studied in Ref. 12 was less than $2 \times 10^{12}\,\mathrm{cm}^{-2}$ with concomitant C_Q values of the order of $10\,\mu\mathrm{F/cm}^2$, which seem to be comparable with the values calculated in this article. In Ref. 13, they fabricated experimental MOSFET-like devices using a graphene sheet and analyzed their data. Accordingly, there was no need to consider sub-band contributions, but for our purposes, counting contributions of several tens of all relevant sub-bands are critical and that is what will be performed below.

We modeled MWCNT characteristics, in accordance with the previous experiments which used such ensembles (with average individual MWCNT diameter of 20 nm and spacing 200 nm on a 5 mm × 5 mm Si substrates) as electrodes.[8,11] We calculated the DoS of a constituent wall in a MWCNT, following previous methodology,[10,14] modeled as a rolled graphene sheet (infinite in the y-direction and both periodic and finite in the orthogonal x-direction). It was assumed that the walls are independent of each other,[15] with the implication that the total DoS can be obtained as the sum of the DoS for each constituent wall. We considered zigzag CNTs (involving rolling of the graphene sheet in the x-direction), as this category encompasses both semiconducting and metallic CNTs.[16] As we consider relatively large diameter CNTs,[11] the details as to how graphene is rolled to yield CNTs, i.e., whether zigzag or armchair or chiral,[17] will not influence C_Q. The exact dispersion relation for a graphene sheet, through the tight-binding approximation[10,18] is

$$E(k_x,k_y) = \pm\gamma_1\sqrt{1+4\cos\left(\frac{\sqrt{3}ak_y}{2}\right)\cos\left(\frac{ak_x}{2}\right)+4\cos^2\left(\frac{ak_x}{2}\right)}. \tag{3}$$

In the above equation, $a = \sqrt{3}a_0$ where a_0 ($= 0.142$ nm) is the C-C bond length and the overlap integral $\gamma_1 = 2.9$ eV.[15] The 20 nm MWCNT with 15 walls was *approximately* indexed through [N, 0] (with $N = 250$ for the outermost wall, and decreasing by 10 for each successive inner wall), and was effectively one dimensional since $k_{x,n} = \frac{2q\pi}{Na}$ (q: sub-band index), while k_y is continuous. The DoS for a single sub-band is then $\frac{4}{2\pi}\frac{dk_y}{dE}$ with $k_{x,n}$ held constant, and the 4 in the numerator accounted for the electron spin degeneracy and the positive/negative k_y.

Since C_Q is a function of E_F from Eq. (1), we needed to estimate an appropriate value for E_F. In a graphene sheet *with no impurities*, each carbon atom provides one electron to the p_z orbital, yielding semi-metallic behavior and implying[19] $E_F = 0$ eV, and zero carrier density (n) at $T = 0$ K. However, n could range around $4.6 \times 10^{12}\,\mathrm{cm}^{-2}$, corresponding to the two-dimensional carrier density interpolated from the experimental value for bulk graphite[15] of $10^{19}\,\mathrm{cm}^{-3}$, i.e., through $(10^{19})^{2/3}$. With variability in n, e.g., due to defects,[13] etc., attempting an exact E_F would yield imprecise values, and it could then be appropriate to estimate n by approximating the CNTs as sheets of graphene and calculating the DoS, as was

done here. The n of $4.6 \times 10^{12}\,\mathrm{cm}^{-2}$ is then only posited as a representative number for the purpose of illustrating the concepts. The actual n in any sample could either be below *or* above[20] this number with a corresponding decrease/increase in C_Q.

From the total carrier concentration at the Fermi energy, $n(E_F) = \int_0^\infty D(E)f(E)dE$. The $f(E)$ is the Fermi-Dirac function and was approximated as a step function in our calculations, as the difference between the value of $f(E)$ with a finite temperature ($T = 300\,\mathrm{K}$) and with $T = 0\,\mathrm{K}$ was at most 5%. The E_F values were found to range around 105 meV (with $n = 4.6 \times 10^{12}\,\mathrm{cm}^{-2}$). Computing E_F ($k_{x,n}$, k_y) from Eq. (3), and then $C_Q(k_{x,n}, k_y)$ from Eq. (1), pairs of E_F and C_Q for all sub-bands $k_{x,n}$ over the Brillouin zone for k_y are plotted in Fig. 2(b). $C_Q(E_F)$ is constant initially due to the metallic CNTs, up to $\sim E_F = 50$ meV, due to the constituent metallic CNTs with finite and constant DoS, where C_Q does not increase as there is no sub-band contribution from the CNTs. The staircase like structure in the variation results from the contribution of successive sub-bands to the DoS. At $E_F = 105$ meV we estimate, in units of capacitance per CNT length, $C_Q = 13$ fF/μm. The linearity in the plot justifies starting with the graphene E_F-k relation to estimate the E_F of the CNT from n.

We next consider the two major components, which add in series, of C_{dl}: (i) a *Helmholtz* capacitor (C_H) due to a Coulombic attraction, and (ii) a *Gouy-Chapman* (C_{GC}) capacitor due to the diffusive distribution of ions in the electrolyte.[3] An area average C_H value can be computed from a spatial separation corresponding to the ionic radius[11] (e.g., $r \sim 0.278$ nm for K^+ ions in $K_3Fe(CN)_6$) and is equal to ε/r. The C_{GC} value is estimated from the voltage drop (ϕ) across the diffusive region (which is of the order of the Debye length, d) and is equal to $(\varepsilon/d)\cosh(e\phi/2k_BT)$. Consequently,

$$\frac{1}{C_{dl}} = \frac{r}{\varepsilon} + \frac{d}{\varepsilon}\frac{1}{\cosh\left(\frac{e\phi}{2k_BT}\right)}. \tag{4}$$

At smaller ϕ ($\rightarrow 0$) $C_{dl} \rightarrow C_{GC}$, at ϕ ($\sim 3k_BT$) C_H and C_G are comparable, and at a larger ϕ ($> 10k_BT$), $C_{dl} \rightarrow C_H$. With a range of ϕ from zero to 105 mV (corresponding to the E_F), we estimate from Eq. (4) a range of C_{dl} for an electrolyte concentration, I (in moles/m^3), from $\sim 7.3\sqrt{I}\,\mu\mathrm{F/cm}^2$ to $\sim 255\,\mu\mathrm{F/cm}^2$. In order to compare to the one-dimensional quantum capacitance C_Q estimated above, we convert the units of C_{dl} by multiplying by $2\pi r$, where $r = 10$ nm is the outer MWCNT wall radius. The corresponding range is then from $4.6\sqrt{I}$ fF/μm to 160 fF/μm. For a given I, say 3 mM as in the experiments (see Table V of Ref. 11), C_{dl} is calculated to be 7.9 fF/μm. With $C_Q = 13$ fF/μm, this results in $C_{tot} \sim$ 4.9 fF/μm. Generally, the electrostatic interaction between surfaces of different geometries decays with a characteristic decay length equal to the Debye length.[21] Equivalent capacitance values are then obtained for the planar/cylindrical cases.

The capacitance per projected electrode area is the product of the obtained C_{tot} value, the average CNT length, $=100\,\mu$m, and the estimated CNT density on the substrate, $\sim 2.5 \times 10^9\,\mathrm{cm}^{-2}$, yielding an expected capacitance value per projected area of $\sim 1200\,\mu\mathrm{F/cm}^2$. Dividing this value by the weight of the CNTs ($\sim 40\,\mu$g), the capacitance values, in F/g, were computed and are shown in comparison to the experimental values (details have been previously reported[8,11]) in Fig. 3. The figure then indicates the relative magnitudes of C_Q relevant to the measured capacitance values and indicates variable C_Q, being more significant (for a series combination of C_{dl} and C_Q) at lower electrolyte concentrations when the CNT is sufficiently isolated so that its DoS is small. We generally observe from the figure that while higher electrolyte concentrations may be adequately modeled through the use of C_{dl} alone, lower concentrations need C_Q as well. C_Q is significant when the CNT is sufficiently isolated so that its DoS is small. As I increases, charge transfer between CNT and electrolyte may be more likely, reducing isolation and increasing the CNT DoS effectively so that C_Q increases and becomes insignificant, as per Eq. (2).

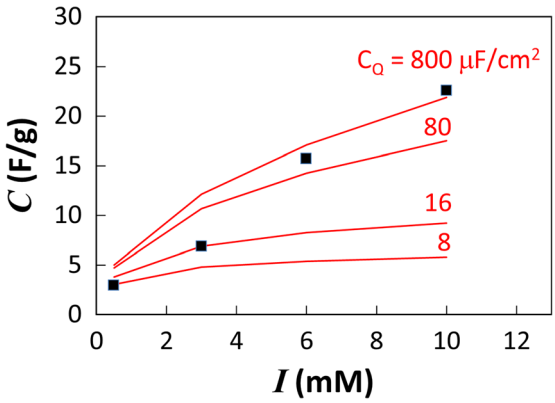

FIG. 3. Comparison of experimentally measured capacitance (see Ref. 11) (■) with numerical estimates (red lines) of C_Q, as a function of electrolyte concentration, I. $C_Q = 20\,\mu\mathrm{F/cm}^2$ corresponds to the theoretically predicted $C_Q = 13$ fF/μm. The agreement is strongest for low I with low C_Q and for high I with high C_Q.

Several insights are obtained through our analyses. For example, the magnitudes of both C_Q and C_{dl} are comparable and suggest an explanation for the considerable (up to 300%) increase in C_{tot} when the CNT constituted electrodes are subject to argon plasma processing.[8,11] Such exposure was hypothesized to introduce charged acceptor like defects into the CNT's carbon lattice, through argon abstracting electronic charge from the carbon bonds. Much like surface states in semiconductors,[22] the fixed charges in the CNT lattice are immobile, and do not respond to applied voltage and would not contribute directly to C_{dl}. However, the added charge density (which would be proportional to the exposure time) affects the Fermi energy and enhances C_Q. A higher C_Q closer to C_{dl} enhances the maximum C_{tot} value that could be obtained from a given system. We can also conclude that the limits to the magnitude of the capacitance value that can be obtained from CNT or nanostructure based electrochemical capacitors are a function of the series combination of *both* the electrostatic/double layer capacitor as well as the quantum capacitor. In a situation where both are comparable, one would need to increase the quantum capacitance value, say through varying the charge density, in order to maximize total capacitance.

This work was supported by the US National Science Foundation under Grant ECS-0643761. The authors thank Professor P. M. Asbeck for useful discussions, as well as Dr. M. Hoefer and Professor P. Yu for relevant comments.

[1]J. R. Miller and A. F. Burke, Electrochem. Soc. Interface **17**, 53 (2008).
[2]J. M. Miller, *Ultracapacitor Applications* (The Institution of Engineering and Technology, Herts, UK, 2011).
[3]A. J. Bard and L. R. Faulkner, *Electrochemical Methods: Fundamentals and Applications*, 2nd ed. (John Wiley, New York, 2001).
[4]A. Peigney, C. Laurent, E. Flahaut, R. R. Basca, and A. Rousset, Carbon **39**, 507 (2001).
[5]P. Simon and Y. Gogotsi, Nature Mater. **7**, 845 (2008).
[6]L. R. Radovic, in *Carbons for Electrochemical Energy Storage and Conversion Systems*, edited by F. Beguin and E. Frackowiak (CRC Press, New York, 2010).
[7]B. E. Conway, J. Electrochem. Soc. **138**, 1539 (1991).
[8]M. Hoefer and P. R. Bandaru, Appl. Phys. Lett. **95**, 183108 (2009).
[9]J. A. Nichols, H. Saito, M. Hoefer, and P. R. Bandaru, Electrochem. Solid State Lett. **11**, K35 (2008).
[10]S. Datta, *Quantum Transport: Atom to Transistor* (Cambridge University Press, New York, 2005).
[11]M. Hoefer and P. R. Bandaru, J. Appl. Phys. **108**, 034308 (2010).
[12]T. Fang, A. Konar, H. Xing, and D. Jena, Appl. Phys. Lett. **91**, 092109 (2007).
[13]J. Xia, F. Chen, J. Li, and N. Tao, Nat. Nanotechnol. **4**, 505 (2009).
[14]L. Forro and C. Schonenberger, in *Carbon Nanotubes-Topics in Applied Physics*, edited by M. S. Dresselhaus, G. Dresselhaus, and P. Avouris (Springer-Verlag, Heidelberg, 2001), Vol. 80.
[15]R. Saito, G. Dresselhaus, and M. S. Dresselhaus, Phys. Rev. B **61**, 2981 (2000).
[16]P. R. Bandaru, J. Nanosci. Nanotechnol. **7**, 1239 (2007).
[17]R. Saito, M. Fujita, G. Dresselhaus, and M. S. Dresselhaus, Appl. Phys. Lett. **60**, 2204 (1992).
[18]C. Beenakker, Rev. Mod. Phys. **80**, 1337 (2008).
[19]M. I. Kastnelson, *Graphene: Carbon in Two Dimensions* (Cambridge University Press, Cambridge, UK, 2012).
[20]D. K. Efetov and P. Kim, Phys. Rev. Lett. **105**, 256805 (2010).
[21]J. N. Israelachvili, *Intermolecular and Surface Forces*, 3rd ed. (Academic Press, San Diego, 2011).
[22]J. Bardeen, Phys. Rev. **71**, 717 (1947).